ARTICLE

A Stable Fuzzy-Based Computational Model and Control for Inductions Motors

Yongqiu Liu[1], Shaohui Zhong[2,*], Nasreen Kausar[3], Chunwei Zhang[4,*], Ardashir Mohammadzadeh[4] and Dragan Pamucar[5,6]

[1]School of Mechanical and Electrical Engineering, Guangdong University of Science & Technology, Dongguan, 523083, China

[2]School of Information, Hunan Open University, Changsha, 410081, China

[3]Department of Mathematics, Faculty of Arts and Sciences, Yildiz Technical University, Esenler, Istanbul, 34220, Turkey

[4]Multidisciplinary Center for Infrastructure Engineering, Shenyang University of Technology, Shenyang, 110870, China

[5]Faculty of Organizational Sciences, University of Belgrade, Belgrade, 11000, Serbia

[6]College of Engineering, Yuan Ze University, Taoyuan, 320315, Taiwan

*Corresponding Authors: Shaohui Zhong. Email: zshtech_1234@sina.com; Chunwei Zhang. Email: zhangchunwei@sut.edu.cn

ABSTRACT

In this paper, a stable and adaptive sliding mode control (SMC) method for induction motors is introduced. Determining the parameters of this system has been one of the existing challenges. To solve this challenge, a new self-tuning type-2 fuzzy neural network calculates and updates the control system parameters with a fast mechanism. According to the dynamic changes of the system, in addition to the parameters of the SMC, the parameters of the type-2 fuzzy neural network are also updated online. The conditions for guaranteeing the convergence and stability of the control system are provided. In the simulation part, in order to test the proposed method, several uncertain models and load torque have been applied. Also, the results have been compared to the SMC based on the type-1 fuzzy system, the traditional SMC, and the PI controller. The average RMSE in different scenarios, for type-2 fuzzy SMC, is 0.0311, for type-1 fuzzy SMC is 0.0497, for traditional SMC is 0.0778, and finally for PI controller is 0.0997.

KEYWORDS

Sliding mode control; self-tuning type-2 fuzzy systems; inductions motor; parameters uncertainty

1 Introduction

In recent years, the application of variable structure strategy using sliding mode control in ac drive systems has attracted much attention. The reasons are due to the main advantages of this method such as insensitivity to change parameters, unaffected by external errors, fast dynamic response, and simplicity of design and execution [1–5]. Basically, in a system controlled by the sliding mode control method, the mode path consists of two parts: the arrival mode and the sliding mode. Before reaching the existing control's switching level (arrival mode), direct the system to the desired level. Sliding mode

occurs when all modes are on the screen. In sliding mode, the dynamic behavior of the system is determined based on the switching plane and is independent of external uncertainties and errors. In practice, limiting the switching frequency causes system modes to remain on the switching surface and fluctuate around it [6]. These oscillations are called chattering, which is undesirable because it increases the control activity and excites the high-frequency dynamics of the system (which are not modeled). So you have to think of a way to fix it.

In [7], to fix the chattering problem, a PID controller was placed in the output of the sliding mode controller. Although the phenomenon of chattering was reduced by using the PID controller, it seems that the use of this controller has reduced the speed of the sliding mode controller, and an important advantage of the sliding mode controllers, namely their response, has not been used. Also, since a non-ideal observer or derivative was used to obtain the acceleration signal, the observer was sensitive to changes in system parameters and the derivative amplifies the noise. The speed control function does not have the desired shape. In [8,9], sliding mode speed controllers with an integrated switching surface were designed in which acceleration information was not required to control the speed. In these references, to solve the chattering problem, a continuous function has been used instead of the signal function in the control signal. However, a high level of uncertainty must be available in the design of this controller. The assumed uncertainties include load torque and changes in the mechanical parameters of the system, which are difficult to measure in practice, so it is difficult to determine the above limit. On the other hand, this parameter is the coefficient of the signal function or its continuous function in the control signal and plays an important role in the occurrence of chattering and its magnitude. In this paper, after ignoring all uncertainties except load torque, an attempt is made to calculate the amount of torque by an adaptive algorithm instantaneously. This method does not give a good answer and the speed step response has a large overshoot. The issue of determining the upper bound of uncertainties remains [10,11]. Since determining the upper bound of uncertainty in sliding mode control is important and necessary, various methods have been presented in the articles for this topic [12–17]. In [18], a neural network was used to estimate the uncertain upper bound of sliding surfaces. Unfortunately, the method presented in the mentioned article requires much information about the system and its parameters, so it is not very efficient in practice. In [19], the type-1 fuzzy system was used to determine the bounded of the sliding-mode control (SMC) surface, and the vehicle suspension system was controlled with it. In the mentioned article, the fuzzy rules and membership functions were not defined correctly, and the chattering phenomenon was observed in the simulation results. In [20], the type-1 fuzzy system was used to determine the upper bound of the sliding mode surface to control the permanent magnet synchronous motor (PMSM). The rules and parameters of the fuzzy system presented in the previous paper are considered fixed and unchanged, and this problem has reduced the efficiency of their method. In recent years, it has been shown that type-2 fuzzy systems have higher capabilities and more efficiency than type-1 ones [21–23]. The type-2 fuzzy system has been used in combination with the SMC method with different methods [24–27]. In [28], some unknown coefficients in sliding mode control have been calculated by the type-2 fuzzy system. In [29], the type-2 fuzzy system was used to calculate one of the parameters of the sliding model method for wind turbine control. The type-2 fuzzy system proposed in the mentioned article is not self-tuning and has a fixed structure. One of the challenges of the sliding mode method is the need to know the mathematical model of the system, so a type-2 fuzzy system can be used to estimate the nonlinear terms of the system model [30]. In [31], type-2 fuzzy control and sliding mode control were used in parallel form for a two-link robot. In other words, in the mentioned article, both controllers do their separate work and therefore type-2 fuzzy system does not calculate the parameters of the sliding mode control. It should be noted that in some articles (such as [30]), it is claimed that there is no need to know the upper bound

of uncertainty, but the methods proposed in these articles do not have a solid mathematical foundation and the stability of the control method is not guaranteed. As seen in the articles with the same title above, in none of those works with type-2 fuzzy neural network, the uncertain upper limit was not calculated in the sliding mode method, and therefore our proposed method is introduced for the first time. The innovations of this article are as follows:

1. Presenting a new mechanism of self-adjusting type-2 fuzzy neural networks for online calculation of uncertain upper limit in sliding mode control method.
2. Convergence proof of the proposed control method.
3. Development and application of the proposed method in an induction motor with real parameters.

The structure of the paper is as follows: first, the dynamics of the induction motor is described, and then the sliding mode control method is presented. In the following, while introducing the fuzzy self-adjustment system, how to use it is explained. Convergence proof of the control system, simulation and conclusion are respectively the last sections of the paper.

2 Induction Motor Drive System

The electromagnetic model for a three-phase induction motor, star connection and squirrel cage in the wheel reference device with synchronous speed is as follows:

$$\frac{di_{ds}}{dt} = -\left(\frac{R_s}{L_\delta} + \frac{R_r L_m^2}{L_r^2 L_\delta}\right) i_{ds} + \omega_e i_{qc} - \frac{R_r L_m}{L_r^2 L_\delta}.\varnothing_{dr} + \frac{\omega_r L_m}{L_r L_\delta}\varnothing_{qr} + \frac{1}{L_\delta}v_{ds} \tag{8}$$

$$\frac{di_{qs}}{dt} = -\omega_e i_{ds}\left(\frac{R_s}{L_\delta} + \frac{R_r L_m^2}{L_r^2 L_\delta}\right) i_{qs} - \frac{\omega_r L_m}{L_r L_\delta}\varnothing_{dr} + \frac{R_r L_m}{L_r^2 L_\delta}\varnothing_{gr} - \frac{1}{L_\delta}v_{qs} \tag{2}$$

$$\frac{d\varnothing_{qr}}{dt} = \frac{R_r L_m}{L_r}i_{ds} - \frac{R_r}{L_r}\varnothing_{dr} - (\omega_e - \omega_r)\varnothing_{qr} \tag{3}$$

$$\frac{d\varnothing_{qr}}{dt} = \frac{R_r L_m}{L_r}i_{qs} - (\omega_e - \omega_r)\varnothing_{qr} - \frac{R_r}{L_r}\varnothing_{qr} \tag{4}$$

where i, $\varnothing$, v, R and L represent current, flux, voltage, resistance and inductance, respectively. The s and r indexes are used to indicate the stator and rotor. The indexes of d and q also specify the components in the dual-axis reference system. ω_r and ω_e are the angular velocities of the rotor and stator, respectively, L_m and L_δ are also mutual and scattering inductances.

$$\left(L_\delta = L_s - \frac{L_m^2}{L_r}\right)$$

The torque produced by the motor and the governing mechanical equations are expressed as follows:

$$T_e = \frac{3PL_m}{4L_r}\left(\varnothing_{dr}i_{qs} - \varnothing_{qr}i_{ds}\right) \tag{5}$$

$$J\frac{d\omega_m}{dt} + B\omega_m + T_L = T_e \tag{6}$$

The parameters of B and J are the coefficient of friction and the inertia constant of the machine, respectively. By using the indirect method, we will ideally have vector control [8]

$$T_e = K_t i_{qs} \tag{7}$$

$$K_t = \frac{3P}{4} \left(\frac{L_m^2}{L_r} \right) i_{ds}^* \tag{8}$$

$$\omega_e = \omega_r + \frac{R_r i_{qs}^*}{L_r i_{ds}^*} \tag{9}$$

Note that i_{qs}^* is torque current command and i_{ds}^* is flux current command. According to the above block diagram relationships, the speed control system is shown in Fig. 1. The position control system is quite similar to the speed control system. The only difference is in the feedback signals on which the speed controller must generate the i_{qs}^* current command signal. In the position control system, in addition to the speed signal, the position signal is also required. We will address this issue in later sections.
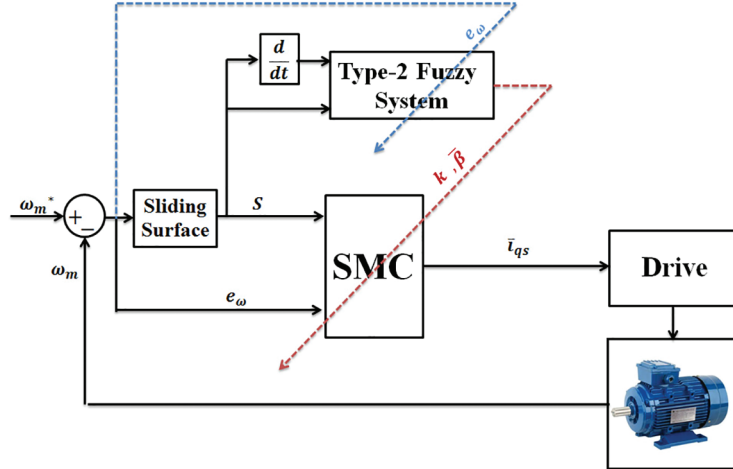

Figure 1: The block diagram of the proposed control system

2.1 Sliding Mode Speed Controller

The mechanical Eq. (6), assuming the existence of uncertainties, can be considered as follows:

$$\dot{\omega}_m(t) = (a + \Delta a)\,\omega_m(t) + (b + \Delta b)\,i_{qs}(t) + (d + \Delta d)\,T_L \tag{10}$$

$$a = -\frac{B}{J}, b = \frac{K_t}{J}, d = \frac{-1}{J}$$

Note that Δa, Δb and Δd are the uncertainties produced by the system parameters K_t, B, J. Now we define the speed error state variable.

$$e_\omega(t) = \omega_m(t) - \omega_m^* \tag{11}$$

where ω_m^* is the speed command. Derived from the parties of Eq. (11) and used (10) in it, the dynamic system of velocity error is obtained as follows:

$$e_\omega(t) = ae_\omega(t) + b\left[i_{qs} + e(t)\right] \tag{12}$$

Note that $e(t)$ is the sum of the uncertainties and is expressed as follows:

$$e(t) = \frac{\Delta a}{a}\omega_m(t) + \frac{\Delta b}{b}i_{qs} + \frac{(d + \Delta d)}{b}T_L \tag{13}$$

$$\bar{i}_{qs}(t) = i_{qs}(t) + \frac{a}{b}\omega_m^* \tag{14}$$

Based on system (12), we propose the following switching levels for speed and position control systems [2].

2.2 Switching Surface Design

The switching level used for the speed control system is as follows [2]:

$$S(t) = h\left[e_\omega(t) - \int_0^t (a + bk)\, e_\omega(\tau)\, d\tau - e_\omega(0)\right] = 0 \tag{15}$$

where h is a positive constant and the login is linear feedback. As can be seen, only the speed error signal is sufficient to calculate the value of S. The following switching level is also recommended for the position control system:

$$S(t) = h\left[e_\omega(t) - (a + bk)e_\omega(t)\right] = 0 \tag{16}$$

Which we have in the position control system:

$$e_\theta(t) = \theta_m(t) - \theta_m^* \tag{17}$$

where θ_m^* is the position command signal and in this system:

$$\dot{\omega}_m = \dot{\theta}_m^* \tag{18}$$

If the state path of system (12) is kept on the switching surface (15), i.e., $S(t) = \dot{S}(t) = 0$, then the dynamic behavior of the speed control system with respect to uncertainties $\Delta a\omega_m(t)$, $\Delta bi_{qs}(t)$ and the load error T_L is not sensitive and follows the following relation:

$$\dot{e}_\omega(t) = (a + bk)\, e_\omega(t) \tag{19}$$

And in the case of the position control system, we will have zero in relation to S (16):

$$e_\omega(t) = \dot{e}_\theta = (a + bk)\, e_\theta(t) \tag{20}$$

Systems (19) and (20) are linear, and by placing the poles of these systems in the left hemisphere (with proper determination of k), the velocity and position errors converge exponentially to zero.

2.3 Speed Controller Design

Based on the mentioned switching levels, we are interested in finding a control that meets the arrival condition and ensures the existence of a sliding mode. For this purpose, we recommend the following speed controller for both levels.

$$\bar{i}_{qs}(t) = ke_\omega(t) - \beta sgn(S(t)) \tag{21}$$

$sgn(0)$ is a function of the sign, β is the upper bound of uncertainties. That is mean:

$$|e(t)| \leq \beta \tag{22}$$

The torque current control, or the output of the speed controller ($i_{qs}^*(t)$), can be obtained by placing (21) in (14). To prove the stability of switching surfaces in both speed and position control modes, write:

$$S(t)\dot{S}(t) = S(t)\{h\dot{e}_\omega(t) - h(a+bk)e_\omega(t)\} = S(t)$$

$$\{ha\dot{e}_\omega(t) + hb\bar{i}_{qs}(t) + hbe(t) - hae_\omega(t) - hbke_\omega(t)\}$$

$$= S(t)\{hbke_\omega(t) - hb\beta Sgn(S(t)) + hbe(t) - hbke_\omega(t)\}$$

$$= bh(e(t)S(t) - \beta|S(t)|) \le -hb|S(t)|(\beta - |e(t)|) \le 0$$

Therefore, the condition of the sliding mode has been met in [9]:

$$S\dot{S} \le 0 \tag{23}$$

The problem here is determining β. From Eq. (13), it can be seen that measuring this parameter is a difficult task. On the other hand, in relation (21), β is the coefficient of the sign function, meaning that this parameter can play an effective role in the occurrence of chattering and its magnitude. Note that the indistinct magnitude of this parameter causes chattering, even if the control signal uses a continuous function instead of a signal function. In the next section, we propose a fuzzy sliding mode controller in which a fuzzy inference mechanism is used to estimate the upper bound of uncertainties.

3 Fuzzy Sliding Mode Speed Controller

This section introduces a self-tuning type-2 fuzzy neural network for estimating the upper bound of uncertainties. First, we replace β with $\bar{\beta}$ in Eq. (21):

$$\bar{i}_{qs}(t) = ke_\omega(t) - \bar{\beta}sgn(S(t)) \tag{24}$$

The estimated value is the upper bound of uncertainties by the fuzzy mechanism. According to Eq. (22) β is a positive value, so $\bar{\beta}$ must also be positive. In the following, we present a new approach to $\bar{\beta}$ other than the high limit of uncertainties. Eq. (24) shows that $\bar{\beta}$ is the amount of control gain applied to the system to direct system states to the switching level. In other words, if S is positive (i.e., the motor speed is higher than the reference value), Eq. (24) will look like this:

$$\bar{i}_{qs}(t) = ke_\omega(t) - \bar{\beta} \tag{25}$$

That is, control over the system is reduced by as much as $\bar{\beta}$. We know that the above signal is the command of the torque generator, and its reduction will reduce the output torque and consequently reduce the speed. This will cause a speed error and then an S value to move to zero. But if S was negative,

$$\bar{i}_{qs}(t) = ke_\omega(t) + \bar{\beta} \tag{26}$$

As a result, the applied control is added to the system and increases the speed. According to Eqs. (25) and (26), it can be seen that in both cases, the size $\bar{\beta}$ determines the amount of control applied to the system. This problem can be used to determine $\bar{\beta}$. It is clear that the farther the system modes are from the surface or in other words, the larger the size S, the more gain control we must apply to the system to prevent the modes from moving away from the surface and returning them. If the value of $\bar{\beta}$ is placed correctly, so that the states of the system move from any point to the switching surface, it can be said that $\bar{\beta}$ was originally the upper bound of uncertainties. Based on the above explanations,

we propose a fuzzy inference mechanism for the proper determination of $\overline{\beta}$. This mechanism estimates $\overline{\beta}$ based on the values of S and $\dot{S}$. The type-2 fuzzy system is defined as follows. Note that N means negative, Z and ZE mean zero, P means positive, PS means positive small, PM means positive medium, PB means positive big and PVB means positive very big.

The type-2 fuzzy membership functions for S and $\dot{S}$ are tuned online. The five fuzzy rules are also expressed as follows:

$$IF \left\{ \left(S \, is \, \tilde{P} \, AND \, \dot{S} \, is \, \tilde{P} \right) or \left(S \, is \, \tilde{N} \, AND \, \dot{S} \, is \, \tilde{N} \right) \right\} \qquad THEN \, \beta \, is \, PVB$$

$$IF \left\{ \left(S \, is \, \tilde{P} \, AND \, \dot{S} \, is \, \tilde{Z} \right) or \left(S \, is \, \tilde{N} \, AND \, \dot{S} \, is \, \tilde{Z} \right) \right\} \qquad THEN \, \beta \, is \, PB$$

$$IF \left\{ \left(S \, is \, \tilde{P} \, AND \, \dot{S} \, is \, \tilde{N} \right) or \left(S \, is \, \tilde{N} \, AND \, \dot{S} \, is \, \tilde{P} \right) \right\} \qquad THEN \, \beta \, is \, PM$$

$$IF \left\{ \left(S \, is \, \tilde{Z} \, AND \, \dot{S} \, is \, \tilde{P} \right) or \left(S \, is \, \tilde{Z} \, AND \, \dot{S} \, is \, \tilde{N} \right) \right\} \qquad THEN \, \beta \, is \, PS$$

$$IF \left\{ \left(S \, is \, \tilde{Z} \, AND \, \dot{S} \, is \, \tilde{Z} \right) \right\} \qquad THEN \, \beta \, is \, ZE$$

The fuzzy output $\overline{\beta}$ can be numerically quantified by the mass center method. So:

$$\overline{\beta} = \frac{\sum_{i=1}^{5} W_i C_i}{\sum_{i=1}^{5} W_i} = \frac{[c_1 \ldots c_5] \begin{bmatrix} y_1 \\ \vdots \\ y_5 \end{bmatrix}}{\sum_{i=1}^{5} y_i} = C^T Y \tag{27}$$

where c_i is the centers of the output membership functions and $C = [c_1, \ldots, c_5]^T$, where y_i is the output membership functions. The problem is to properly determine the vector C. In the simulations, we will show that the improper value of this parameter causes β not to be estimated correctly. It seems that it is better to determine this vector according to the operating conditions of the motor (distance or proximity of the states to the switching surface) and change it in different conditions. This is done in the next section using an adaptive algorithm. Fig. 1 shows the block diagram of the proposed control system.

As seen in Fig. 1, the control system is very new and can control and manage any changes in the system with an online adaptive algorithm. In Eqs. (25) and (26), it was observed that the parameters k and $\overline{\beta}$ should be determined in the sliding mode control system. This is done by the type-2 fuzzy system so that the error tends to 0. To avoid confusing the readers, the updated equations of type-2 fuzzy system are not presented.

3.1 Stability Analysis

In this section, an adaptive algorithm is proposed to optimally determine the estimated value. This algorithm modifies and optimizes membership function centers according to the conditions. The algorithm used is [11]:

$$\dot{C} = ahb \, |S| \, Y \tag{28}$$

Note that a is a positive number and is estimated by the fuzzy system at every moment. As can be seen, the value of S and the degree of membership of the relevant rule are effective in calculating the

membership center. Assume that $\hat{\beta}$ is the optimal value for estimating the error. In the previous part, we saw that:

$$\hat{\beta} = \hat{C}^T Y \tag{29}$$

C is the optimal vector corresponding to β. The error value of the above vector is defined as follows.

$$\check{C} = C - \hat{C} \tag{30}$$

To prove the stability of the mentioned algorithm, we choose the following Lyapunov function:

$$V = \frac{1}{2}\left(S^2 + \frac{1}{\alpha}\check{C}^T \tilde{C}\right) \tag{31}$$

Derived from V with respect to time we have:

$$\dot{V} = S\dot{S} + \frac{1}{a}\tilde{C}^T\dot{C} = S\left(h\left[\dot{e}_\omega - (a+bk)\,e_\omega\right]\right) + \frac{1}{\alpha}\tilde{C}^T\dot{C}$$

$$= hS\left(ae_\omega + b\bar{i}_{qs} + be - ae_\omega - bke_\omega\right) + \frac{1}{\alpha}\tilde{C}^T\dot{C}$$

$$= hS\left(bke_\omega - b\beta sgn\,(s) + be - bke_\omega\right) + \frac{1}{\alpha}\tilde{C}^T\dot{C} \leq -hb\,|S|\,(\beta - |e|) + \frac{1}{\alpha}\tilde{C}^T\dot{C}$$

$$= -hb\,|S|\left(\hat{\beta} - |e| + \beta - \hat{\beta}\right) + \frac{1}{\alpha}\tilde{C}^T\dot{C} = -hb\,|S|\left(\hat{B} - |e| + \beta - \hat{\beta}\right) + \frac{1}{\alpha}\tilde{C}^T\dot{C}$$

$$= -hb\,|S|\left(\hat{\beta} - |e|\right) - hb\,|S|\,\tilde{C}^T Y + \frac{1}{\alpha}\tilde{C}^T\dot{C}$$

$$= -hb\,|S|\left(\hat{\beta} - |e|\right) - \frac{1}{\alpha}\tilde{C}^T\left(\dot{C} - \alpha hb\,|S|\,Y\right)$$

Once Eq. (28) is established, the above result will be less than zero and the function will be stable.

4 Simulation

The induction motor used in the simulation is 0.8 kW and has the following specifications [2]:

Rated speed: rpm2000

Nominal stator voltage: v120

Nominal value J∗: 0.000676 N.m.s²/rad

Number of poles: 2

Nominal stator current: 5.4 A

Nominal value B∗: 0.000515 N.m.s²/rad

The current controller is a PI controller and its output is voltage commands. To implement these commands, the SVPWM (Space Vector Pulse Width Modulation) method with a switching frequency of 4 kHz has been used [10]. Applying the signal function to the speed controller causes chattering, which we have used to reduce the following softened function:

$$\bar{i}_{qs} = Ke_\omega\,(t) - \beta\frac{S\,(t)}{|S\,(t)| + \delta} \tag{32}$$

δ is a small positive constant and here 1/1 is chosen. Selecting the control signal ensures that the states are superimposed only in a narrow band around the switching plane. In other words, the value of S will not necessarily be zero. This should be considered in the design of an adaptive algorithm. Because S is not zero, the adaptive algorithm is always active and constantly increases β, which causes chattering. Therefore, in selecting α, we proceed as follows:

$$\alpha = \begin{cases} 0 & |S| \le \delta \\ \alpha_0 & |S| > \delta \end{cases} \tag{33}$$

α_0 is a positive number and is equal to 10 selected here.

To control the speed of the block, the diagram in Fig. 1 has been completely simulated and the answers of different controllers have been obtained for both starting and loading modes of the motor. The figures show the two basic variables, speed and output of the speed controller. The speed diagram shows the control capability and i_{qs}^* indicates the amount of control activity performed. For all i_{qs}^* current controllers, it is limited to 15 A. At first, the reference speed is considered sinusoidal. In Fig. 2, you can see the performance results of four type-2 fuzzy-based SMC (proposed in this article), type-1 fuzzy-based SMC, traditional SMC (with fixed parameters) and PI.
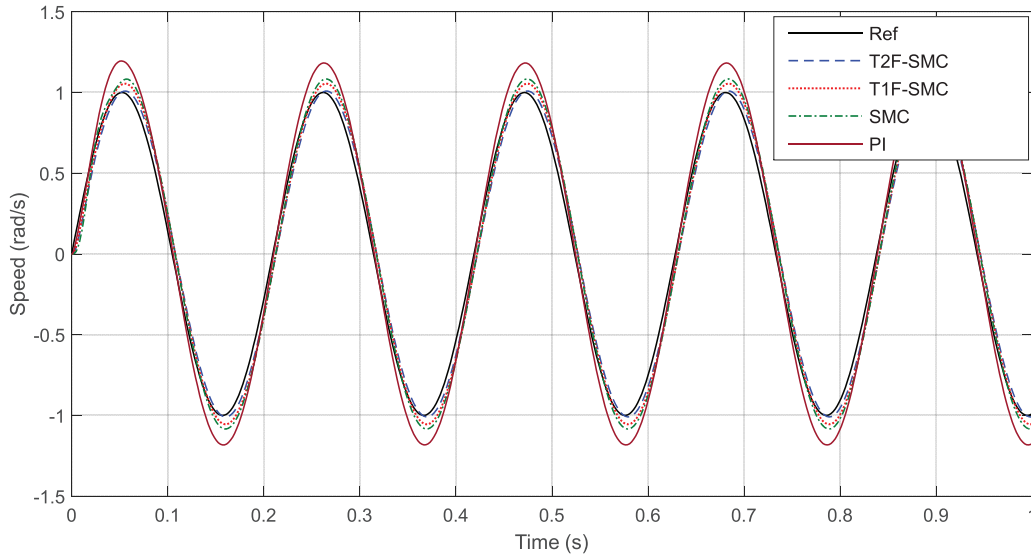
Figure 2: Performance of control systems in sinusoidal reference speed tracking

As can be seen in Fig. 2, the best performance is firstly SMC based on type-2 fuzzy, secondly SMC based on type-1 fuzzy, thirdly traditional SMC and finally PI. At peak motor speed, the performance difference is more obvious. In the following, the performance of the control systems has been measured by applying the load torque $T_L = 1\,Nm$ at the moment $t = 0.45\,s$ (Fig. 3).

In Fig. 4, for more clarity, the part of Fig. 4 where the load torque is applied is shown enlarged.

Since applying momentary load torque is one of the conventional methods of challenging electric motor control systems, a larger load torque ($T_L = 4\,Nm$) has been applied to the motor (Fig. 5).

In Fig. 6, for more clarity, the part of Fig. 5 where the load torque is applied is enlarged.

As can be seen in Fig. 6, in the PI controller, after applying the load torque, the motor speed suddenly drops from 0.9 to 0.3 rad/s, which is not a good performance at all. Also, for SMC, it goes from about 0.75 rad/s to less than 0.6 rad/s.

Another way to evaluate the performance of control systems is to examine the step response (Figs. 7 and 8).
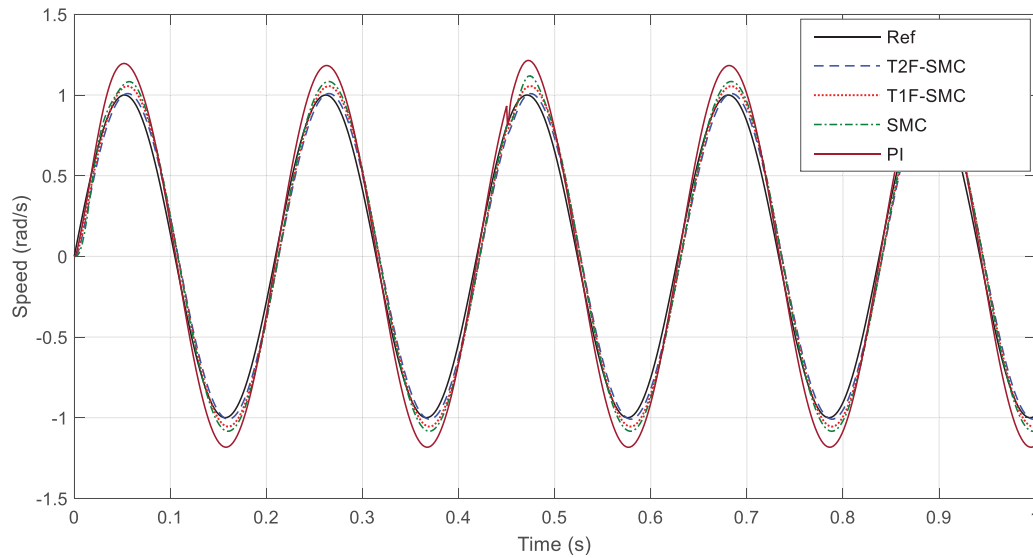

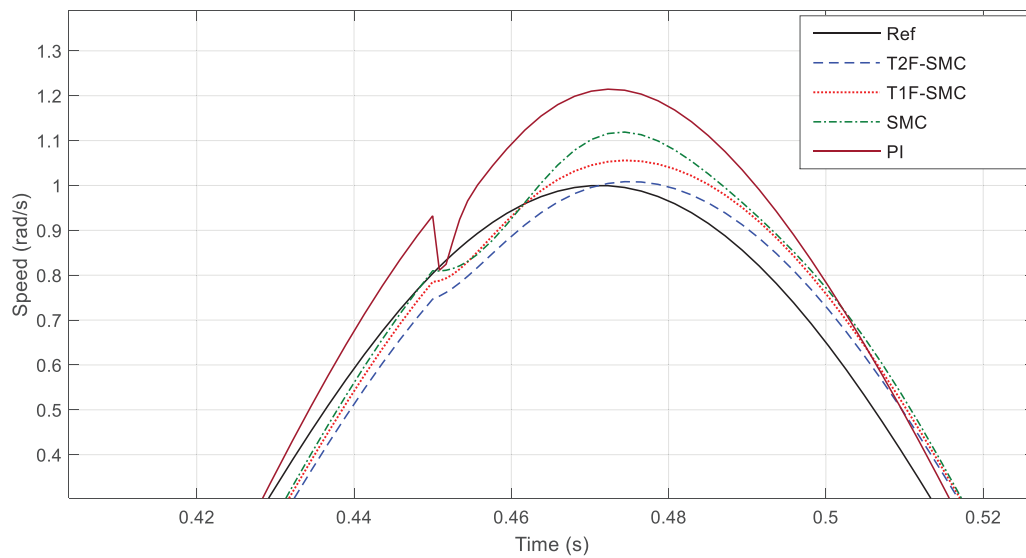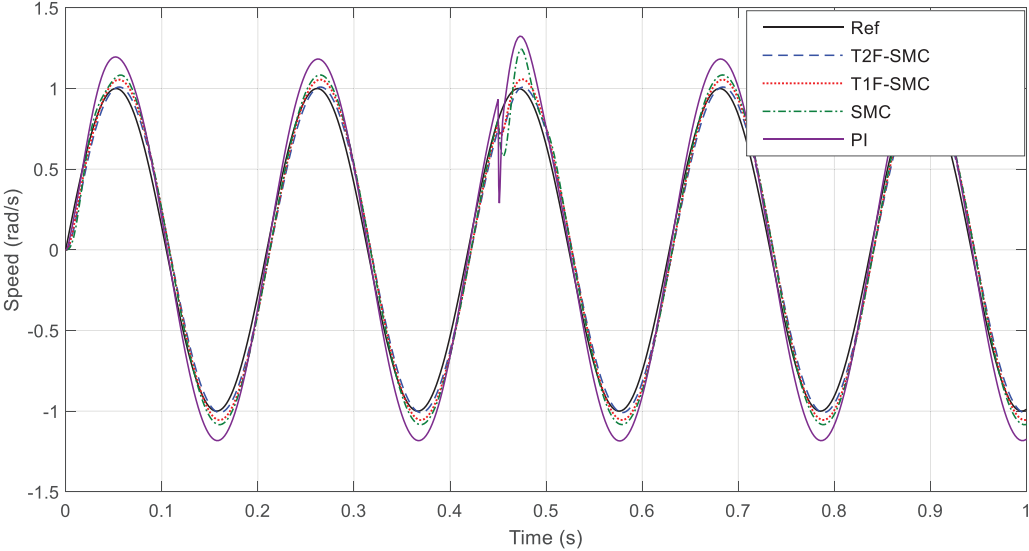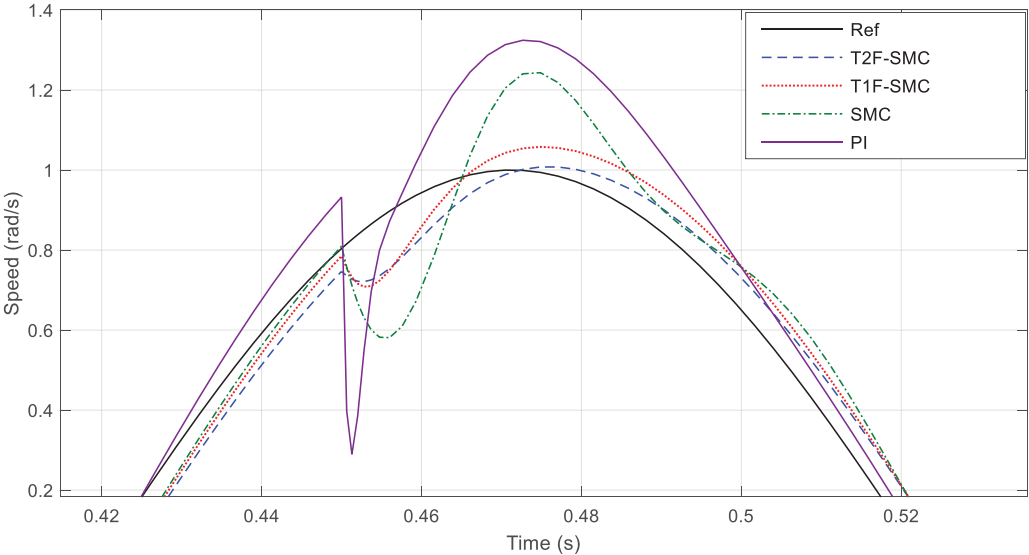**Figure 3:** Performance of control systems in sinusoidal reference speed tracking by applying load torque $T_L = 1\,Nm$ at $t = 0.45\,s$

Figure 4: Enlargement of the area of Fig. 4 where the load torque is applied

Figure 5: Performance of control systems in sinusoidal reference speed tracking by applying load torque $T_L = 4\,Nm$ at $t = 0.45\,s$

Figure 6: Enlargement of the area of Fig. 6 where the load torque is applied
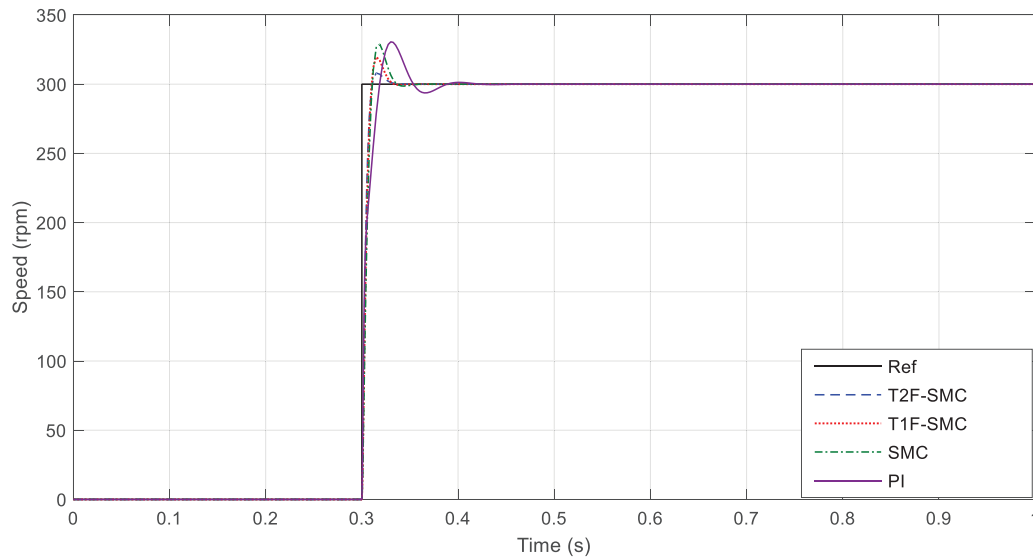
Figure 7: Performance of control systems in step reference speed tracking
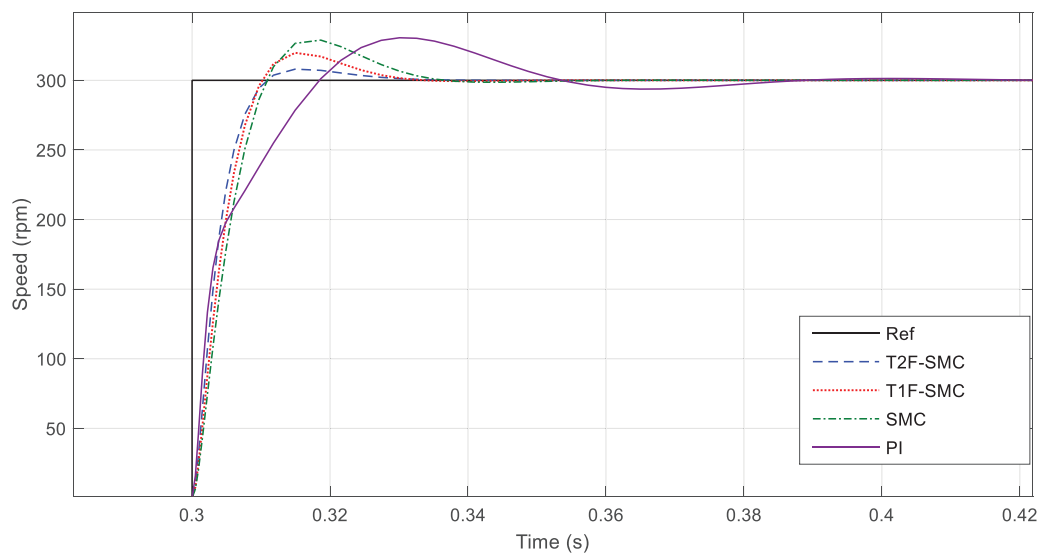
Figure 8: Enlargement of an area of Fig. 7

As it is clearly seen in Fig. 8, the type-2 fuzzy-based SMC has minimum overshoot and it has reached the final value with the minimum possible time. In the following, it is assumed that a load torque of $T_L = 1\,Nm$ is applied at moment $t = 0.5\,s$ and removed at moment $t = 0.75\,s$ (Figs. 9 and 10).
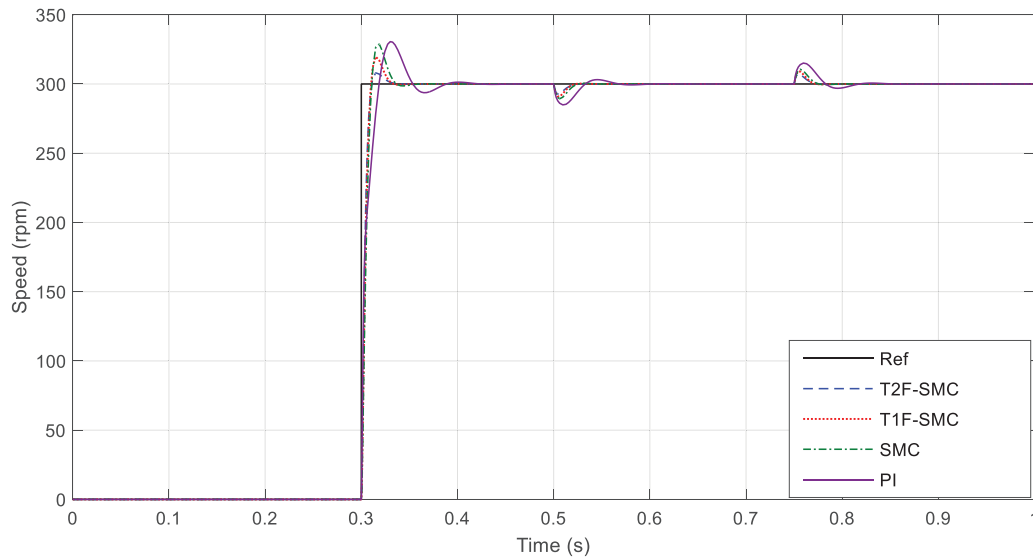
Figure 9: Performance of control systems in step reference speed tracking by applying load torque $T_L = 1\,Nm$ at $t = 0.5\,s$ and removing it at $t = 0.75\,s$
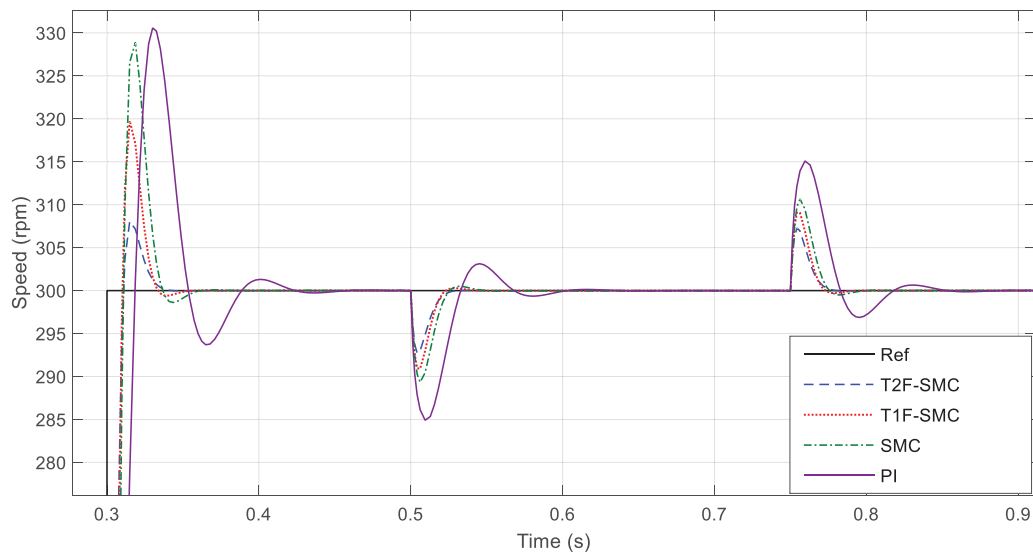
Figure 10: Enlargement an area of Fig. 9

Fig. 10 clearly shows the effect of the type-2 fuzzy system in improving SMC performance. This controller has been able to control the motor with minimum oscillation and maximum speed both at the moment of applying the load torque and at the moment of removing it. Another fundamental challenge for evaluating the control system is the variation of motor parameters (R_s, R_r, L_m, L_r, L_δ, J, B). At first, it is assumed that at the moment $t = 0.5\,s$, the parameters will double at once (Fig. 11).

As can be seen from Fig. 11, the proposed control system has the best performance in the face of doubling parameters. In Fig. 12, it is assumed that the parameters of the motor are halved at once.
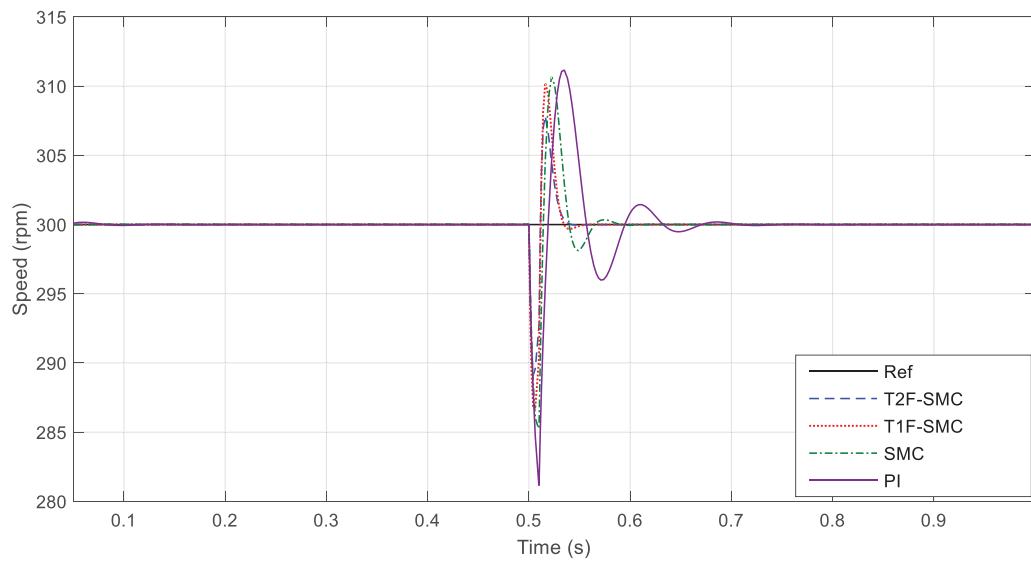
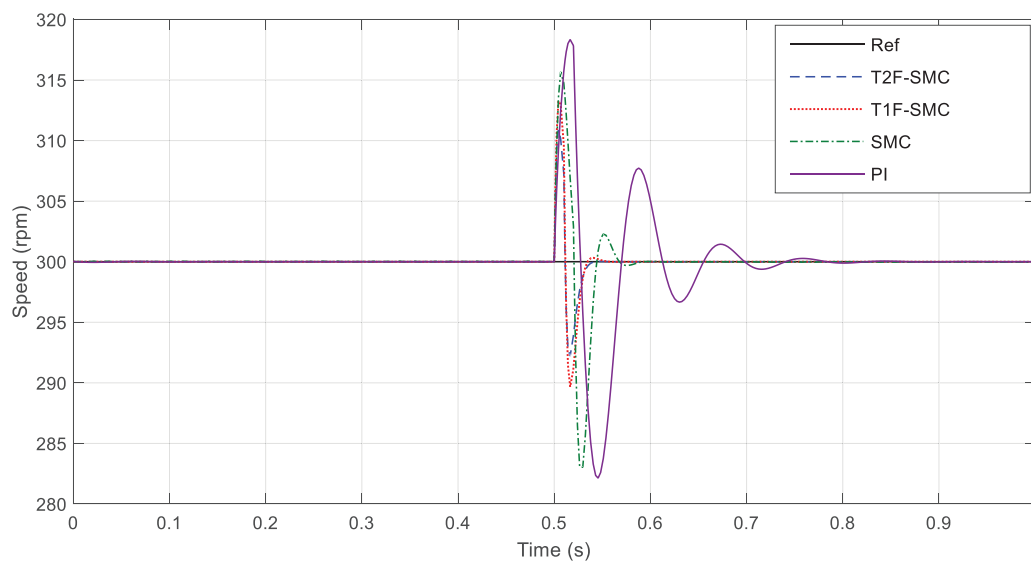**Figure 11:** Performance of control systems in the face of doubling parameters

Figure 12: Performance of control systems in the face of halving parameters

It can be seen in Fig. 12 that the halving of the parameters has challenged the control system more. Therefore, in the following, it is assumed that the parameters of the motor will be quartered at once (Fig. 13).
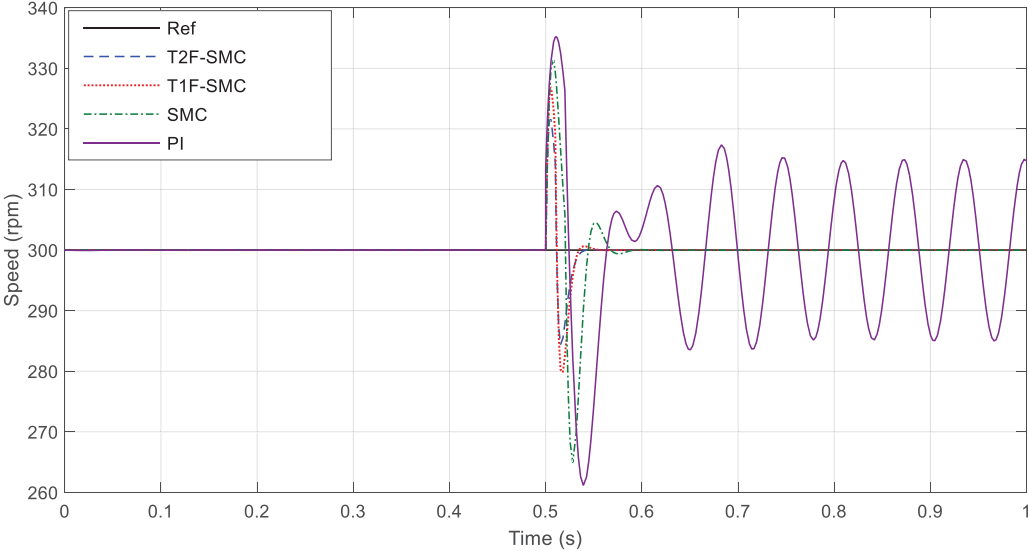
Figure 13: Performance of control systems in the face of quartering parameters

Figs. 13 and 14 show interesting results. It can be seen that the PI controller loses its efficiency when faced with large changes in parameters. Of course, this result was expected because the PI controller coefficients are constant and cannot respond in case of drastic changes in the system. In the case of the other three control systems, the importance of using the fuzzy system to online adjust the SMC is clearly evident. Figs. 15 and 16 show the control system's performance in stator current and torque control for step response (Fig. 7), respectively.
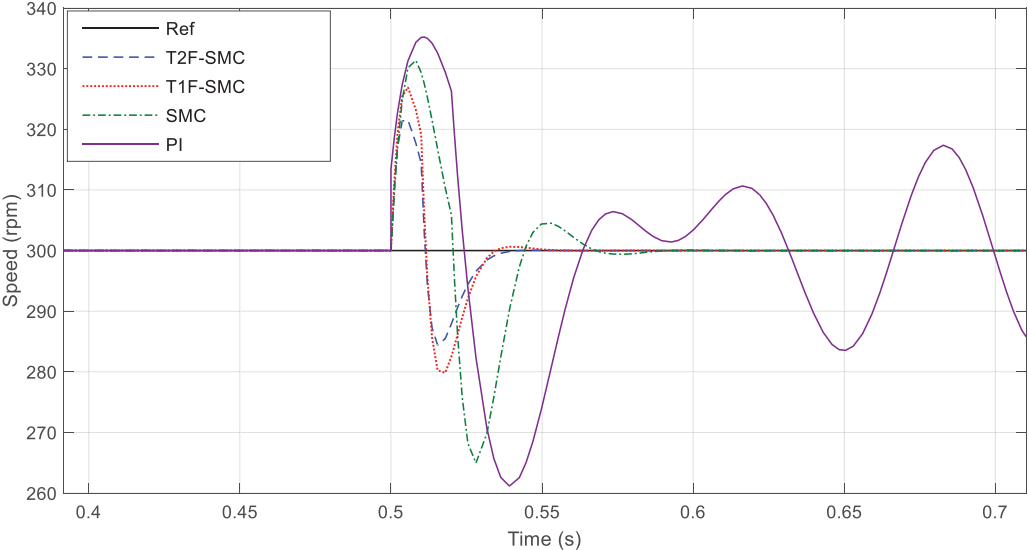

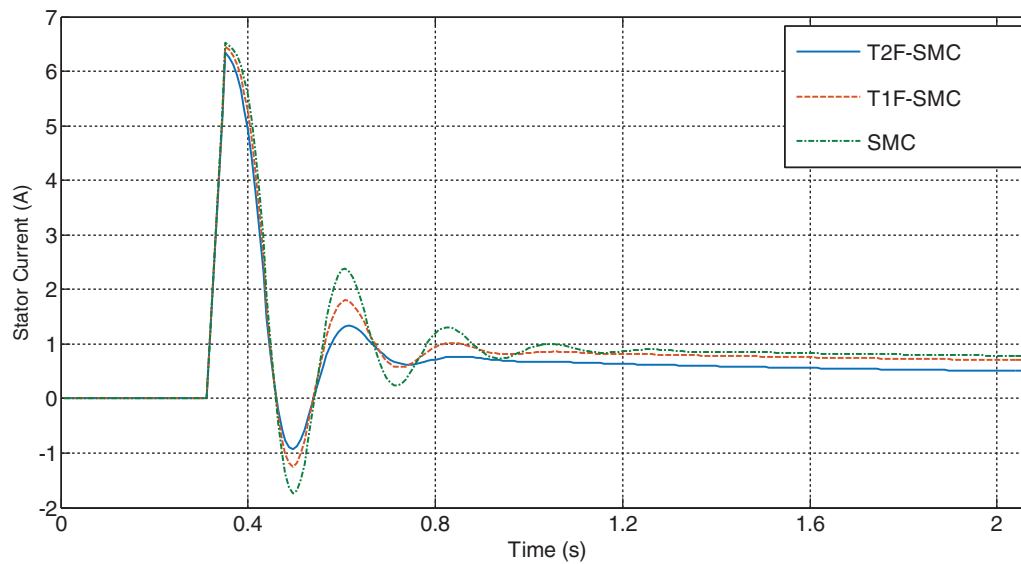**Figure 14:** Enlargement of an area of Fig. 13

Figure 15: Performance of the control system in stator current control
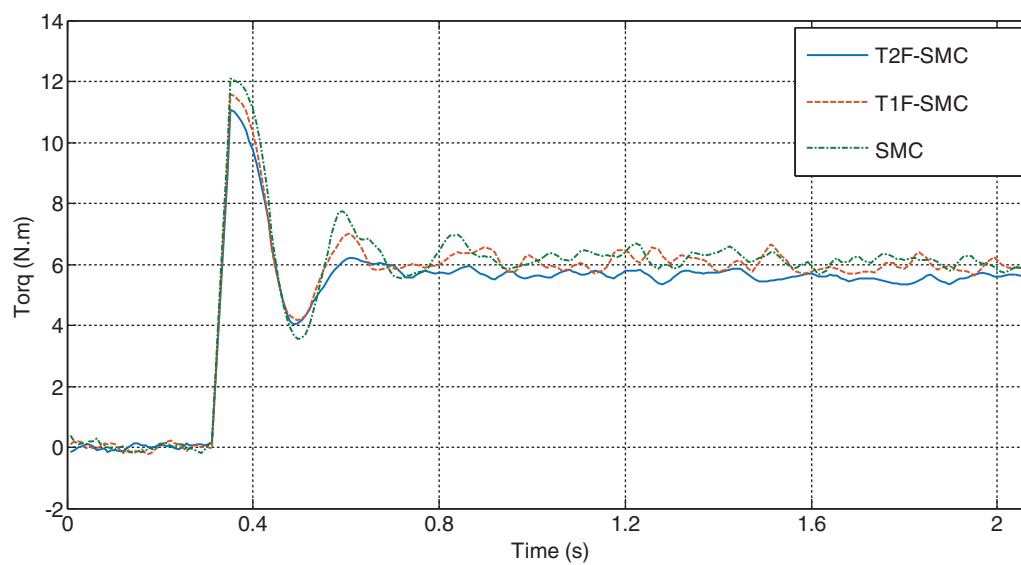

Figure 16: Performance of the control system in torque control

According to the results, the proposed control system has better performance than the other two methods. Also, Figs. 17 and 18 show the performance of the control system to tracking the PWM signal.
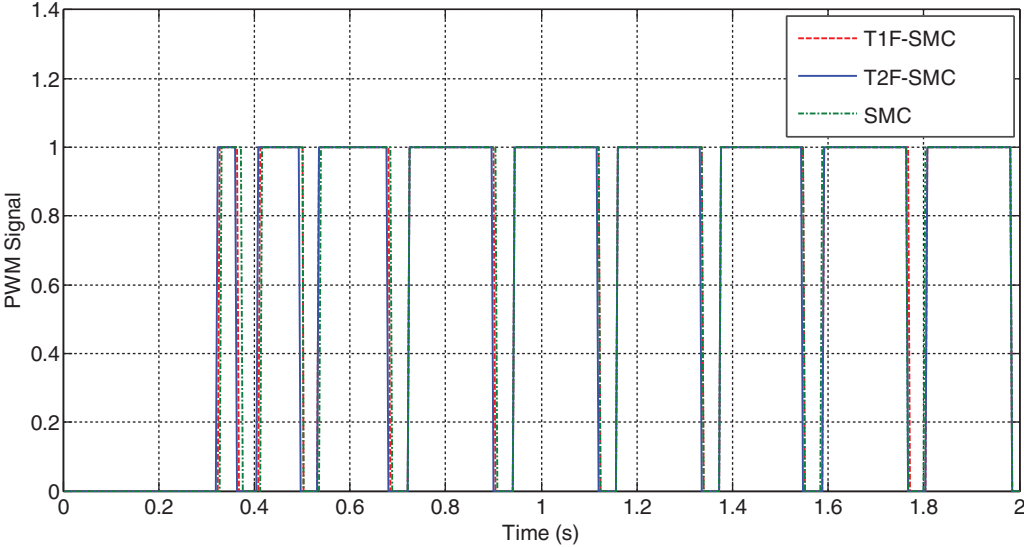
Figure 17: Performance of the control system in tracking the PWM signal
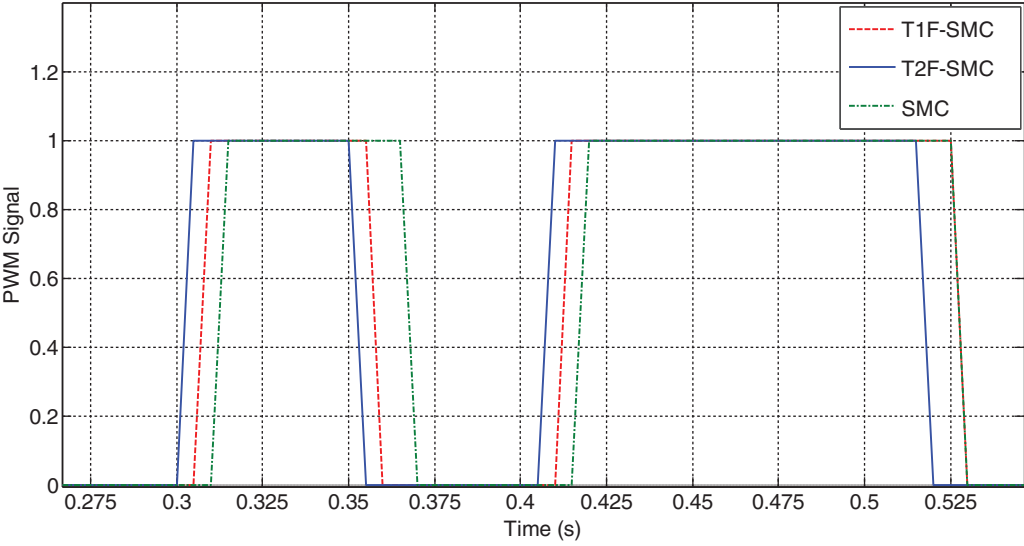

Figure 18: Enlargement of an area of Fig. 17

Table 1 shows the average RMSE in different scenarios.

As can be seen from Table 1, the proposed method has the best performance among other methods. The suggested approach can be improved using developed fuzzy systems and optimal control scenarios [32–37].

Table 1: Comparison of the proposed method with other methods

Control method	RMSE
Type-2 fuzzy SMC (proposed method)	0.0311
Type-1 fuzzy SMC	0.0497
Traditional SMC	0.0778
PI controller	0.0997

5 Conclusion

In this article, a new method for setting and updating SMC parameters based on type-2 fuzzy system was presented. SMC is a robust and widely used controller in all kinds of uncertain systems. One of the weaknesses of this control system is that its parameters are fixed. This problem is exciting for time-varying systems or systems whose dynamics change over time. In this paper, a type-2 fuzzy system performed the task of online adjustment and updating of SMC parameters well. By applying the load torque and uncertain parametric types in the simulation, the proposed method came out with pride. The RMSE for type-2 fuzzy SMC was 0.0311, and for type-1 fuzzy SMC was 0.0497. For traditional SMC was 0.0778, and finally, for PI controller was 0.0997. As suggestions to continue this research, it is possible to use type-3 fuzzy, which has been used a lot recently.

Conflicts of Interest: The authors declare that they have no conflicts of interest to report regarding the present study.

References

1. Zhang, J., Meng, W., Yin, Y., Li, Z., Ma, L. et al. (2022). High-order sliding mode control for three-joint rigid manipulators based on an improved particle swarm optimization neural network. *Mathematics, 10,* 3418. https://doi.org/10.3390/math10193418
2. Huang, H., Shirkhani, M., Tavoosi, J., Mahmoud, O. (2022). A new intelligent dynamic control method for a class of stochastic nonlinear systems. *Mathematics, 10(9),* 1406.
3. Shiravani, F., Alkorta, P., Cortajarena, J. A., Barambones, O. (2022). An enhanced sliding mode speed control for induction motor drives. *Actuators, 11,* 18. https://doi.org/10.3390/act11010018
4. Chen, B., Hu, J., Zhao, Y., Ghosh, B. K. (2022). Finite-time observer based tracking control of uncertain heterogeneous underwater vehicles using adaptive sliding mode approach. *Neurocomputing, 481(5),* 322–332.
5. Li, D., Yu, H., Tee, K. P., Wu, Y., Ge, S. S. et al. (2021). On time-synchronized stability and control. *IEEE Transactions on Systems Man Cybernetics-Systems,* 1–14. https://doi.org/10.1109/TSMC.2021.3050183
6. Liu, S., Song, Z., Liu, Y., Chen, Y., Liu, C. (2022). Flux-weakening controller design of dual three-phase PMSM drive system with copper loss minimization. *IEEE Transactions on Power Electronics, 38(2),* 2351–2363. https://doi.org/10.1109/TPEL.2022.3216513
7. Liu, S., Feng, Z., Cai, Y. (2019). Switching frequency regulation in sliding mode control for synchronous buck converter. *The Journal of Engineering, 2019(16),* 1841–1846. https://doi.org/10.1049/joe.2018.8831

8.   Wei, Z., Zhao, M., Liu, X., Lu, M. (2022). A novel variable-proportion desaturation PI control for speed regulation in sensorless PMSM drive system. *Applied Sciences, 12(18),* 9234. https://doi.org/10.3390/app12189234

9.   Tavoosi, J., Shirkhani, M., Azizi, A., Din, S. U., Mohammadzadeh, A. et al. (2022). A hybrid approach for fault location in power distributed networks: Impedance-based and machine learning technique. *Electric Power Systems Research, 210,* 108073.

10. Liu, S., Liu, C. (2021). Virtual-vector-based robust predictive current control for dual three-phase PMSM. *IEEE Transactions on Industrial Electronics, 68(3),* 2048–2058. https://doi.org/10.1109/TIE.2020.2973905

11. Luo, B. Y., Subroto, R. K., Wang, C. Z., Lian, K. L. (2022). An improved sliding mode control with integral surface for a modular multilevel power converter. *Energies, 15,* 1704. https://doi.org/10.3390/en15051704

12. Yadav, S. L., Karvekar, S. S. (2022). Design of integral sliding mode controller for speed control of induction motor. *2022 2nd International Conference on Intelligent Technologies (CONIT)*, pp. 1–6. Hubli, India. https://doi.org/10.1109/CONIT55038.2022.9847959

13. Kochetkov, S., Krasnova, S. A., Utkin, V. A. (2022). The new second-order sliding mode control algorithm. *Mathematics, 10,* 2214. https://doi.org/10.3390/math10132214

14. Zhang, X., Shi, R., Zhu, Z., Quan, Y. (2022). Adaptive nonsingular fixed-time sliding mode control for manipulator systems' trajectory tracking. *Complex & Intelligent Systems,* 1–12. https://doi.org/10.1007/s40747-022-00864-w

15. Hou, M., Tan, F., Han, F., Duan, G. (2019). Adaptive sliding mode control of uncertain nonlinear systems with preassigned settling time and its applications. *International Journal of Robust and Nonlinear Control, 29(18),* 6438–6462. https://doi.org/10.1002/rnc.4729

16. Danyali, S., Aghaei, O., Shirkhani, M., Aazami, R., Tavoosi, J. et al. (2022). A new model predictive control method for buck-boost inverter-based photovoltaic systems. *Sustainability, 14(18),* 11731.

17. Hu, J., Wu, Y., Li, T., Ghosh, B. K. (2019). Consensus control of general linear multiagent systems with antagonistic interactions and communication noises. *IEEE Transactions on Automatic Control, 64(5),* 2122–2127. https://doi.org/10.1109/TAC.2018.2872197

18. Guo, X., Shirkhani, M., Ahmed, E. M. (2022). Machine-learning-based improved smith predictive control for MIMO processes. *Mathematics, 10,* 3696. https://doi.org/10.3390/math10193696

19. Sun, S., Cui, W., Zheng, J. (2022). Robust sliding mode control for stochastic uncertain discrete systems with two-channel packet dropouts and time-varying delays. *Sensors, 22,* 1965. https://doi.org/10.3390/s22051965

20. Yeh, Y. L. (2021). Output feedback tracking sliding mode control for systems with state- and input-dependent disturbances. *Actuators, 10,* 117. https://doi.org/10.3390/act10060117

21. Wen, T., Fang, Y., Lu, B. (2022). Neural network-based adaptive sliding mode control for underactuated dual overhead cranes suffering from matched and unmatched disturbances. *Autonomous Intelligent Systems, 2(1),* 2392. https://doi.org/10.1007/s43684-021-00019-7

22. Li, G., Ruan, Z., Gu, R., Hu, G. (2021). Fuzzy sliding mode control of vehicle magnetorheological semi-active air suspension. *Applied Sciences, 11,* 10925. https://doi.org/10.3390/app112210925

23. Mecifi, M., Boumediene, A., Boubekeur, D. (2021). Fuzzy sliding mode control for trajectory tracking of an electric powered wheelchair. *AIMS Electronics and Electrical Engineering, 5(2),* 176–193. https://doi.org/10.3934/electreng.2021010

24. Wang, Z., Ran, L., Kong, B., Jia, X., Liu, L. et al. (2022). Suspension system control based on type-2 fuzzy sliding mode technique. *Complexity, 2022(21),* 2685573. https://doi.org/10.1155/2022/2685573

25. Zhang, Y., Huang, Y., Zhang, Z., Postolache, O., Mi, C. (2022). A vision-based container position measuring system for ARMG. *Measurement and Control, 56,* 596–605. https://doi.org/10.1177/00202940221110932

26. Liu, S., Liu, C., Zhao, H., Liu, Y., Dong, Z. (2022). Improved flux weakening control strategy for five-phase PMSM considering harmonic voltage vectors. *IEEE Transactions on Power Electronics, 37(9),* 10967–10980. https://doi.org/10.1109/TPEL.2022.3164047

27. Li, B., Tan, Y., Wu, A., Duan, G. (2021). A distributionally robust optimization based method for stochastic model predictive control. *IEEE Transactions on Automatic Control, 67(11),* 5762–5776. https://doi.org/10.1109/TAC.2021.3124750

28. Li, B., Zhou, X., Ning, Z., Guan, X., Yiu, K. C. (2022). Dynamic event-triggered security control for networked control systems with cyber-attacks: A model predictive control approach. *Information Sciences, 612(3),* 384–398. https://doi.org/10.1016/j.ins.2022.08.093

29. Zhong, C., Zhou, Y., Chen, J., Liu, Z. (2022). DC-side synchronous active power control of two-stage photovoltaic generation for frequency support in Islanded microgrids. *Energy Reports, 8,* 8361–8371. https://doi.org/10.1016/j.egyr.2022.06.030

30. Nafia, N., El Kari, A., Ayad, H., Mjahed, M. (2018). Robust interval type-2 fuzzy sliding mode control design for robot manipulators. *Robotics, 7(3),* 40. https://doi.org/10.3390/robotics7030040

31. Roy, S., Baldi, S., Fridman, L. M. (2020). On adaptive sliding mode control without a priori bounded uncertainty. *Automatica, 111,* 108650. https://doi.org/10.1016/j.automatica.2019.108650

32. Tian, J., Hou, M., Bian, H., Li, J. (2022). Variable surrogate model-based particle swarm optimization for high-dimensional expensive problems. *Complex & Intelligent Systems, 406,* 12. https://doi.org/10.1007/s40747-022-00910-7

33. Lukovac, V., Popović, M. (2018). Fuzzy Delphi approach to defining a cycle for assessing the performance of military drivers. *Decision Making: Applications in Management and Engineering, 1(1),* 67–81.

34. Adak, A. K., Kumar, D. (2022). Spherical distance measurement method for solving MCDM problems under pythagorean fuzzy environment. *Journal of Fuzzy Extension and Applications, 2022,* 28–39. https://doi.org/10.22105/jfea.2022.351677.1224

35. Peng, Z., Hu, J., Shi, K., Luo, R., Huang, R. et al. (2020). A novel optimal bipartite consensus control scheme for unknown multi-agent systems via model-free reinforcement learning. *Applied Mathematics and Computation, 369,* 124821. https://doi.org/10.1016/j.amc.2019.124821

36. Anusha, G., Ramana, P. V., Sarkar, R. (2022). Hybridizations of Archimedean copula and generalized MSM operators and their applications in interactive decision-making with q-rung probabilistic dual hesitant fuzzy environment. *Decision Making: Applications in Management and Engineering, 6(1)*. https://doi.org/10.31181/dmame0329102022a

37. Mollaei, M. (2022). Fuzzy metric topology space and manifold. *Journal of Fuzzy Extension and Applications, 2022,* 18–27. https://doi.org/10.22105/jfea.2022.338931.1217